IEEE Access
Multidisciplinary | Rapid Review | Open Access Journal

Received 22 October 2024, accepted 7 November 2024, date of publication 14 November 2024, date of current version 26 November 2024.

Digital Object Identifier 10.1109/ACCESS.2024.3498053

TOPICAL REVIEW

Stimulation-Induced Artifact Removal of the Local Field Potential Through Hardware Design: Toward the Implantable Closed-Loop Deep Brain Stimulation

YI-HUI WU[1], HSIAO-CHUN LIN[1], CHI-WEI HUANG[1], CHUNG-YU WU[1,2], (Life Fellow, IEEE), AND MING-DOU KER[1,2], (Fellow, IEEE)

[1]Biomedical Electronics Translational Research Center, National Yang Ming Chiao Tung University, Hsinchu 300, Taiwan
[2]Institute of Electronics, National Yang Ming Chiao Tung University, Hsinchu 300, Taiwan

Corresponding author: Ming-Dou Ker (mdker@ieee.org)

This work was supported by the National Science and Technology Council (NSTC) in Taiwan under Contract 113-2321-B-A49-018, Contract 112-2321-B-A49-011, Contract 111-2321-B-A49-002, Contract 110-2321-B-009-004, and Contract 109-2221-E-009-100-MY3.

ABSTRACT Deep brain stimulation is a standard neurosurgery to treat advanced Parkinson's disease patients. An innovative technology known as closed-loop deep brain stimulation is under development. This technology aims to identify abnormal biomarker signals within the brain, and create novel systems featuring sophisticated hardware configurations to generate improved therapeutic approaches and more favorable outcomes. The primary challenge faced in advancing closed-loop deep brain stimulation is managing artifacts induced by electrical stimulation within the signal detection module. A notable circuit design challenge involves continuously monitoring local field potential alterations during electrical stimulation. The artifacts arising from the stimulation can be categorized into common-mode artifact voltage and differential-mode artifact voltage. Within this article, a comprehensive review encompasses recent methodologies designed to mitigate common-mode artifact voltage and differential-mode artifact voltage in local field potential through hardware-centric techniques, including filtering, template removal, blanking, and selective sampling. The inherent strengths and limitations of these strategies are compared and discussed. This article allows engineers to recognize appropriate artifact removal techniques to achieve an implantable closed-loop deep brain stimulation system. To this end, a more intelligent and more precise system could be developed for the treatment of Parkinson's disease and other neurological disorders.

INDEX TERMS Closed loop systems, deep brain stimulation, implants, local field potential, Parkinson's disease, stimulation-induced artifact.

I. INTRODUCTION

Parkinson's disease (PD), a prevalent neurodegenerative condition among the elderly, is mainly characterized by motor system impairment within the central nervous system. Cardinal motor manifestations include bradykinesia, rigidity, and resting tremor [1]. The causes of PD are influenced by diverse factors, with genetic and environmental influences exerting their roles. The pathological analysis of patient brain sections has revealed extensive degeneration of dopaminergic cells within the substantia nigra pars compacta (SNc) of the midbrain, giving rise to the apparent motor symptoms [1]. Levodopa stands as the primary pharmacological intervention for PD patients. Nonetheless, extended levodopa usage can result in drug-induced complications like motor fluctuations and dyskinesia [2]. In such situations, recourse to deep brain stimulation (DBS) emerges as a viable treatment strategy [3].

A DBS device comprises distinct elements, including the electrode lead, extension lead, and implantable pulse generator (IPG) [3]. The subthalamic nucleus (STN) is the primary

The associate editor coordinating the review of this manuscript and approving it for publication was Hasan S. Mir.

electrode implantation target. Previous studies have demonstrated that degeneration of dopaminergic cells within the SNc disrupts dopamine regulation within the motor circuit of the basal ganglia, leading to aberrant heightened neural activity within the STN. This, in turn, interferes with the transmission and modulation of action commands originating from the motor cortex [4], [5]. The conventional approach of DBS involves continuously administering a modest level of electrical stimulation. This serves to mitigate the pathologic neural activity within the STN, ultimately ameliorating the motor symptoms associated with PD patients. Common stimulation parameters comprise a stimulation frequency set at 130 Hz, a pulse width of 60 μs, and an optimal stimulation intensity that fosters symptom improvement without immediate adverse reactions. This conventional DBS configuration assumes an open-loop design [6]. The IPG delivers uninterrupted electrical stimulation upon determining the stimulation parameters until the battery becomes exhausted. Accordingly, a subsequent surgical intervention is required to replace the IPG.

Open-loop DBS has been found effective in treating motor symptoms in advanced PD patients. Nevertheless, complaints of stimulation-induced side effects persist. Notable stimulation-induced side effects include postural instability, gait disturbance, and dysarthria [6], [7], [8]. A hypothesis posits that open-loop DBS, while effectively suppressing the pathological neural activity of the STN, also disrupts physiological neural activity [6], [7], [8]. It is presumed that physiological and pathological neural activity should be distinguished. When pathological signals appear, electrical stimulation is applied to suppress neural activity, and when physiological activity is detected, the stimulation intensity can be reduced. This mode of neural activity-guided feedback-controlled stimulation is referred to as a closed-loop design [6], [7], [8]. The closed-loop DBS has verified the potential to enhance the therapeutic efficacy of electrical stimulation, mitigate side effects arising from excessive stimulation, and extend the battery life of the IPG by conserving power [9], [10], [11], [12], [13], [14].

The local field potential (LFP) within the STN of PD patients can be captured using deep brain electrodes [5], [15]. The LFP represents the transient summation of synaptic potentials recorded near the electrode, offering insight into the synchronized activity of neighboring neurons [5], [15]. Within the LFP recordings obtained from the STN of patients with PD, spectral analysis via a fast Fourier transform can be used to examine the spectral distribution. Numerous PD patients exhibit distinctive LFP patterns characterized by one or two prominent peak frequencies falling within the beta band of the 13 to 35 Hz range, commonly referred to as beta oscillations [16]. These beta oscillations in the STN serve as distinctive LFP markers for PD patients. Following the administration of levodopa or activation of DBS stimulation in PD patients, as their motor symptoms ameliorate, the power associated with the peak frequency of beta oscillations tends to decrease or fade. Conversely, beta oscillations reappear as the drug effects diminish or DBS is deactivated [17], [18]. The power magnitude of the peak frequency in STN beta oscillations exhibits a strong correlation with PD symptoms, particularly bradykinesia and rigidity, rendering it a pivotal biomarker for closed-loop DBS [6], [7], [15].

From a hardware design perspective, the IPG of open-loop DBS simply contains a stimulation module. Conversely, additional sensing and control modules are integral components in the closed-loop circuit design for DBS. The sensing module primarily comprises a chip engineered to detect LFP signals, which typically manifest at the microvolt level. To mitigate noise, the use of bipolar electrodes next to the stimulation electrode facilitates the acquisition of differential signals during LFP detection within the STN. After detection, the analog LFP signals are amplified and converted to digital signals. The control module undertakes the processing of digital signals, executed by the biomedical signal processor (BSP) according to the closed-loop stimulation algorithm. Consequently, the outcome of the algorithm governs the control of the stimulation module.

Currently, closed-loop DBS applications in PD treatment tend to employ unused electrodes on the same electrode lead for LFP signal sensing [7], [19]. This approach offers the advantage of allowing the STN, where the electrode lead is implanted, to autonomously detect abnormal LFP without requiring additional surgical procedures, such as inserting a cortical sensing electrode for electrocorticography measurement, to serve as feedback control signals [20]. This conserves the operational process, reducing surgical time and potential complications [7], [19]. However, a significant challenge arises in the form of stimulation-induced artifacts that contaminate the LFP signals, frequently saturating, and rendering them unusable during stimulation. If the input signals saturate at the analog front-end (AFE), subsequent processing within the back-end BSP becomes unfeasible. Even when input signals remain unsaturated, the back-end BSP must endeavor the stimulation-induced artifacts, potentially complicating circuit design and increasing the chip size and power consumption. Therefore, effective stimulation-induced artifact removal at the AFE level becomes crucial, ensuring undistorted LFP signal processing by the back-end BSP.

Closed-loop DBS is regarded as a novel and promising approach for mitigating the adverse effects induced by stimulation in PD patients. However, the sensing module of closed-loop DBS must be able to detect the LFP of the patient's STN, regardless of whether stimulation is active or not. This necessitates the continuous detection of signals, presenting a strict challenge in the development of sensing modules. The AFE analog circuits or back-end BSPs are designed to address the issue of stimulation-induced artifact removal and to prevent the saturation of the LFP sensing module.

For implantable closed-loop DBS, the measured signal must reflect the symptoms, and the processing time and the stimulation trigger time must be short enough to respond to the biomarker. However, in neuroscience, nerve conduction takes time, so clinically, implantable closed-loop DBS would not stimulate within a few microseconds after signal acquisition. The main actions of closed-loop DBS are to capture proper physiological signals (biomarkers), remove stimulation artifacts, and trigger stimulation to treat symptoms.

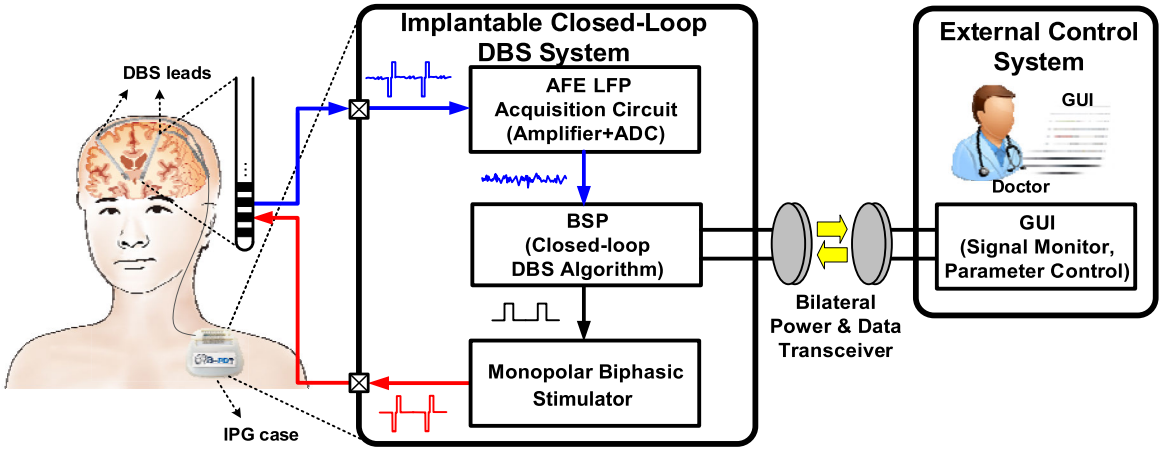

FIGURE 1. System architecture of implantable closed-loop DBS system.

According to [21], in closed-loop DBS, the neural biomarkers of LFP range from 7 Hz to 260 Hz. According to [22], the duration of the stimulation artifact is approximately 0.2 ms before and 4 ms after the artifact peak. According to [23], the beta burst of LFP longer than 600 ms is a meaningful physiological biomarker of PD. Therefore, in the implementation of implantable closed-loop DBS, the delay time from when the biomarker appears in the patient's brain signal to when the system responds by adjusting DBS is 800 ms [24]. If the processing latency is too long, signal processing will be delayed beyond the normal nerve conduction time, causing the signal to fail to reflect physiological symptoms. Suppose the processing latency is too short, and the signal processing needs to be more intensive. In that case, a processor with powerful computing capabilities will be required, increasing energy consumption and making it unsuitable for implantable devices.

This article presents a comprehensive review of stimulation-induced artifacts removal hardware techniques for the guidance of implantable closed-loop DBS design. First, Section II introduces clinical electrophysiological signals, closed-loop DBS systems, and stimulation-induced artifacts. The category and performance of different artifact removal techniques are reviewed in Section III. A comparison of hardware-design-based techniques for artifact removal and optimal implantable closed-loop methods for stimulation-induced artifact removal is suggested in Section IV. Finally, a conclusion is given in Section V.

II. STIMULATION-INDUCED ARTIFACT

The spectrum of LFP typically pertains to a bandwidth of less than 100 Hz and can be categorized into several bands: the delta band (<4 Hz), the theta band (4 to 7 Hz), the alpha band (8 to 12 Hz), the beta band (13 to 35 Hz), and the gamma band (>35 Hz) [5]. The amplitude of LFP is characterized by its smallness, often ranging from several to hundreds of microvolts. In comparison with other prevalent clinical electrophysiological signals like the electroencephalogram (EEG), electrocorticogram (ECoG), electrocardiogram (ECG), and electromyography (EMG), the LFP signal exhibits notably diminutive amplitude (refer to Table 1).

TABLE 1. Comparison of clinical electrophysiological signals.

Electrophysiological signals	Amplitude (mV)	Bandwidth (Hz)	Clinical and research applications
Local field potential (LFP)	0.01 to 1	0.5 to 100	Treatment of Parkinson's disease
Electroencephalogram (EEG)	0.01 to 0.1	0.5 to 100	Seizure detection, the diagnosis of encephalopathy
Electrocorticogram (ECoG)	0.1 to 1	0.5 to 100	Sleep studies, seizure detection, cortical mapping
Electrocardiogram (ECG)	1 to 5	0.05 to 100	Diagnosis of ischemia, arrhythmia, conduction defects
Electromyography (EMG)	1 to 10	20 to 2000	Muscle function, neuromuscular disease prosthesis

The electrode-electrolyte interface represents the localized region between the deep brain electrode and the adjacent neural tissue. The applied current induces localized electrochemical reactions at this interface during electrical stimulation [25]. Inadequate electrode materials or excessive charge density from stimulation can lead to electrode corrosion and increased electrochemical noise, potentially compromising the signal-to-noise ratio of recorded LFPs [26], [27]. Currently, platinum-iridium alloy is employed as the material for deep brain electrodes due to its superior resistance to oxidation and corrosion [26], [28]. Furthermore, the charge density produced by electrical stimulation remains below thresholds that would typically cause significant corrosion [27], [28]. Consequently, despite long-term recordings of abnormal LFPs in PD patients, the contribution of electrode-generated background noise remains minimal.

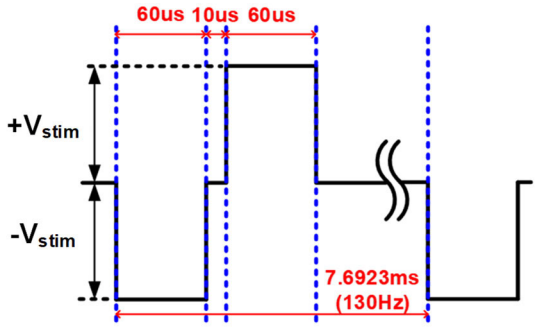

FIGURE 2. Commonly used DBS biphasic square stimulation waveform (a pulse width of 60 μs and a stimulation frequency of 130 Hz).

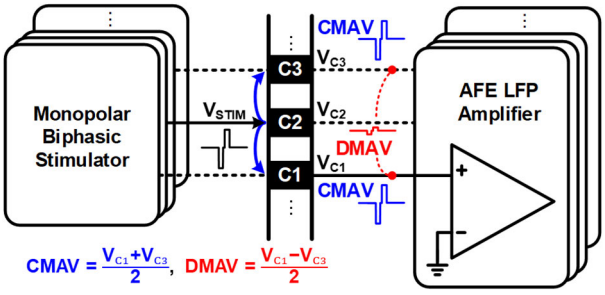

FIGURE 3. Common mode artifact voltage (CMAV) and differential mode artifact voltage (DMAV). [32].

An implantable closed-loop DBS system (depicted in Fig. 1) employs an AFE acquisition circuit to record LFP. Following analog-to-digital conversion (ADC) of the LFP data, the digital signals are conveyed to the BSP, which commands the monopolar biphasic stimulation. After processing via the closed-loop DBS algorithm, the stimulation control based on specific LFP biomarkers is governed by the BSP. Electrical stimulation has two variants: constant voltage stimulation (CVS) and constant current stimulation (CCS). Currently, CCS finds widespread clinical usage due to its smaller residual charge following stimulation, compared to CVS [29].

Typically, the stimulation waveform (as depicted in Fig. 2) assumes a biphasic configuration characterized by negative and positive symmetry to minimize the impact of residual charges on the human body [30]. Thus, the stimulation-induced artifact voltage exhibits negative and positive components ($-V_{stim}$ / $+V_{stim}$). Regardless of the type of electrical stimulation applied, the stimulation process itself gives rise to corresponding artifacts within the AFE acquisition circuit. Due to the shared electrode contacts between the stimulator circuit and the AFE acquisition circuit, stimulation pulses originating from CCS or CVS become coupled to neighboring electrode contacts, thereby introducing stimulation-induced artifact voltages to the AFE acquisition circuit. For this reason, the LFP signals obtained from the AFE acquisition circuit are subject to contamination by these artifact voltages stemming from the stimulation. At the input node of the AFE acquisition circuit, two types of artifact voltages are observed: common-mode artifact voltage (CMAV) and differential-mode artifact voltage (DMAV) [31], as illustrated in Fig. 3 [32].

The presence of a relatively large voltage noise is known as CMAV. CMAV can induce device overload or output saturation within the AFE acquisition circuit. For example, when a stimulation intensity of $\pm$ 3.6 V is applied, an extent CMAV of about $\pm$ 1.2 V may propagate to adjacent electrode contacts [33]. Additionally, DMAV, due to the mismatch artifact voltage, arises from the processes employed to address CMAV. In theory, mitigation of CMAV is achievable by performing signal subtraction within the AFE acquisition circuit, focusing on the instances where the detected signals remain unsaturated. Nonetheless, mismatches usually emerge among signals originating from distinct electrode contacts or brain tissues. After the subtraction, the residual noise stemming from the mismatch in voltage is referred to as DMAV, and then both the differential LFP signals and DMAV experience concurrent amplification by the AFE acquisition circuit. Excessive DMAV magnitude holds the potential to result in saturation of the output signal. Conversely, DMAV also represents a chief contributor to signal distortion within the AFE acquisition circuit. Efforts to remove CMAV and DMAV within the AFE acquisition circuit and to facilitate the accurate recording of LFPs during DBS have prompted the formulation of more effective methodologies. These strategies aim to mitigate artifacts induced by stimulation, thus enhancing the fidelity of signal capture.

III. CATEGORY AND PERFORMANCE OF ARTIFACT REMOVAL TECHNIQUES

Various techniques for artifact removal have been proposed in previous studies, categorized into filtering [31], [34], [35], [36], template removal [33], [37], [38], [39], [40], [41], [42], [43], blanking [44], [45], and selective sampling [22], [32], [46]. A conceptual review of the advantages and disadvantages of each technique, as well as a review of relevant literature, is presented below.

A. FILTERING

Filtering represents an early technique that typically employs analog or digital filters for artifact removal [31], [34], [35], [36]. Two common strategies include the design of a pre-filter before the AFE amplifier to prevent amplifier saturation, and the implementation of a high-order post-filter after the AFE amplifier to remove artifacts (refer to Fig. 4). In terms of spectral characteristics, the stimulation frequency needs to be significantly distant from the frequency band of the detection signal (as illustrated in Fig. 5). Additionally, inadequate filter order might inadvertently lead to the filtration of actual biosignal data or incomplete artifact removal.

In applying the CMAV removal technique with filtering, a common-mode cancellation (CMC) path is employed as described in [34], where positive feedback cancellation is utilized for artifact removal. The common-mode (CM) signals at the electrodes are detected and amplified. At the input stage, these amplified CM signals are differentially subtracted from the original signal ($V_{in,CM}$) via capacitors. It is worth noting that all input circuit voltages must not be overvoltage in this

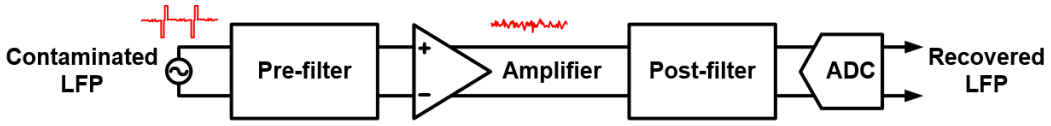

FIGURE 4. Block diagram of filtering designed before the amplifier (pre-filter) and after the amplifier (post-filter).

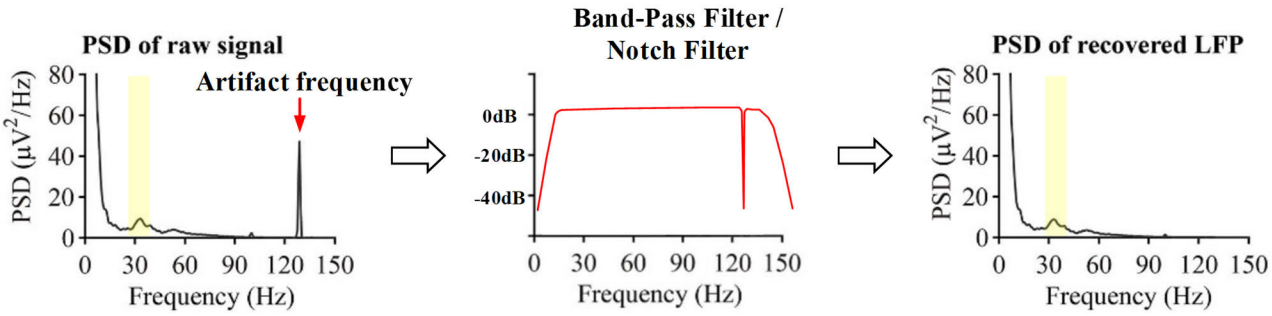

FIGURE 5. A band-pass filter used for stimulation-induced artifact removal of DBS.

technique. A low-gain (26 dB) and high-input range chopper amplifier are used to preserve the neural signals of interest. However, the CMAV allowable range, set at 650 mV_{pp}, is limited and cannot accommodate negative artifact voltages.

In [34], the DMAV removal technique is implemented through post-filtering in digital domain. Following digitization by the ADC, high-order filtering is applied through a digital processor, enabling closed-loop control stimulation. Although a moderate DMAV allowable range of 80 mV_{pp} achievable through filtering exists, it is important to note that the filter circuit is not integrated into the AFE amplifier. An integrated or dedicated post-filtering circuit is not mentioned in this work.

The advantage of filtering lies in its straightforward implementation and capacity to remove artifact voltages within a designated frequency band [22]. Nevertheless, the disadvantage is the increased power consumption associated with high-order filters [22], [47]. Power demands can become significant when implemented in the digital domain, possibly requiring offline operation. Accordingly, filtering may not be suitable for implantable closed-loop DBS system applications. Additionally, filtered biological signals may encounter distortion in the frequency domain. This filtering method is primarily suited for high-frequency stimulation, requiring the stimulation frequency to be substantially distant from the biomarker frequency [47].

B. TEMPLATE REMOVAL

The template removal technique finds widespread usage [33], [37], [38], [39], [40], [41], [42], [43]. It is assumed, in principle, that stimulation-induced artifacts appear as continuous events and that each stimulation-induced artifact waveform exhibits considerable similarity. In this technique, the shape of the stimulation-induced artifact voltages is estimated, either within digital domain or at AFE stage, to create a template, which is subsequently incorporated into a negative feedback mechanism. The template is subtracted from the original signal either within digital domain or at AFE stage. Template removal can be categorized into template removal in digital domain and template removal in analog domain.

1) TEMPLATE REMOVAL IN DIGITAL DOMAIN

The shape of stimulation-induced artifact voltages is derived from the ADC output or another digital domain output to create a digital template. This digital template is subsequently subtracted from the original signal either directly within digital domain or at AFE stage through the digital-to-analog converter (DAC) to restore the signal. Template removal in digital domain technique encompasses two distinct strategies.

First, after signals containing stimulation-induced artifacts are collected, they are amplified through an amplifier and then digitized through an ADC. As shown in Fig. 6(a), the technique involves training a template, subsequently fed back to the input end of the amplifier for artifact removal. This methodology offers the advantage of circumventing potential amplifier saturation issues at the output terminal.

In contrast, as depicted in Fig. 6(b), the other template removal in digital domain technique entails training a template on the digital signal processor after the ADC output, followed by the direct subtraction of signals within digital domain. However, this technique is limited by the possibility of CMAV saturation at the input stage, making any subsequent processing useless.

In [37], the template removal in digital domain technique is utilized to subtract the template from the original signal in the AFE stage through DAC. Given that both the feedback methods of CMAV and DMAV are utilized in the study, the disadvantage is the low CMAV allowable range (1.5 V_{pp}), which restricts its capability to manage negative artifact voltages. Nevertheless, with precise template training, the advantages of a high DMAV allowable range (300 mV_{pp}), elevated precision, rapid filter

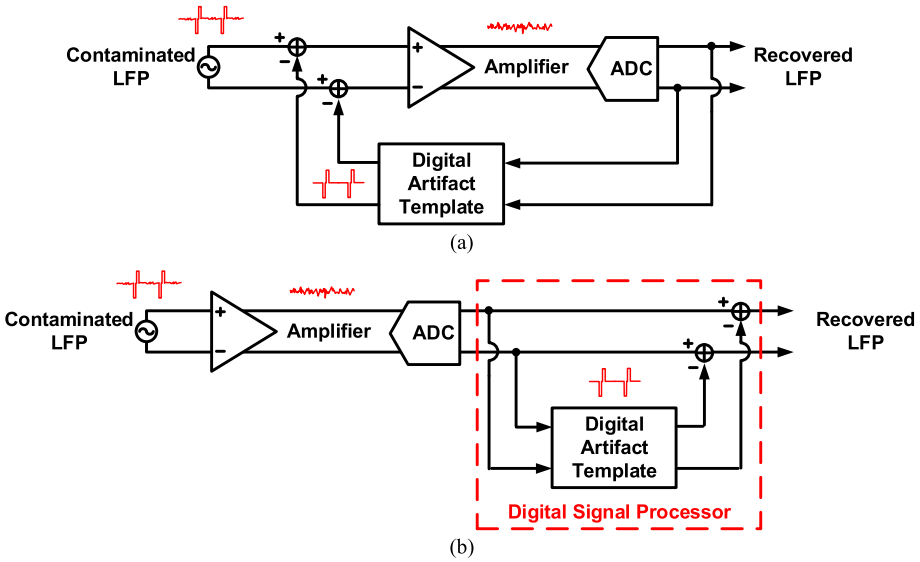

FIGURE 6. Block diagram of template removal in digital domain: (a) subtract the template from the original signal in AFE stage through DAC; (b) subtract the template from the original signal in digital domain directly.

response time, and minimal noise and power consumption are manifested.

In [38], the template removal in digital domain technique is utilized to subtract the template from the original signal in digital domain. In the CMAV removal technique, differential input and differential output are utilized solely. Conversely, in the DMAV removal technique, a voltage-controlled oscillator (VCO) at the input end of the amplifier is used to convert the input voltage signal into the frequency domain. Since the saturation of the stimulation artifact is mainly in the voltage domain, the input voltage signal is converted into the frequency domain. The voltage dictates the oscillation frequency of the VCO. For instance, a higher voltage signal results in a correspondingly elevated oscillation frequency, and vice versa. As a result, both neural signals and artifact voltages can be recorded without encountering output saturation in the frequency domain. This technique additionally furnishes a substantial voltage-to-frequency gain across an extensive input range, with a substantial allowable range for DMAV ($\pm$ 50 mV). After conversion, the frequency domain is reversed to produce a voltage signal. This involves subtracting the template from the initial signal in the digital realm to eliminate the artifact voltage. This method mitigates the saturation of the common-mode signals. However, distortion unavoidably arises during the conversion process from voltage to frequency and back to voltage, reducing overall linearity.

The advantage of template removal in digital domain lies in the potential for achieving high linearity in artifact removal results when the estimated template shape of artifact voltages closely aligns with their original form and demonstrates high consistency [48]. This technique can remove a substantial portion of stimulation-induced artifacts. However, it is accompanied by the disadvantage that the digital template cannot remove CMAV, which could lead to potential output saturation of the AFE amplifiers [22], [47]. Furthermore, even minor estimation errors can produce significant residual artifact voltages in the AFE amplifier output when the template subtraction occurs in the AFE stage. Extended response times may result in signal loss and excessive stimulation. Additionally, the digital processing entails a relatively high computational load and may require a considerable chip area for an additional digital template. Enhanced estimation accuracy demands offline operation, rendering it unsuitable for implantable closed-loop DBS system applications.

2) TEMPLATE REMOVAL IN ANALOG DOMAIN

The template removal in analog domain technique involves estimating the shape of the stimulation-induced artifact voltage within the AFE stage to create an analog template. The analog circuitry generates the artifact voltage template before the ADC. Template training is achieved using analog filters or comparators. Within the AFE stage, the original signal undergoes a subtraction operation with the analog template to retrieve the signal in the temporal domain (Fig. 7). This technique offers the advantage of accommodating both CMAV and DMAV processing within the AFE, ensuring that the AFE amplifier remains free from saturation. Thus, the template removal in analog domain technique proves more suitable for implantable closed-loop DBS applications. Nonetheless, this method requires a more intricate circuit design to address asymmetric DMAV.

In [33], a high-voltage chopper circuit featuring clamping diodes is predominantly utilized for CMAV removal. The primary operational principle involves the initial passage of the stimulation-induced artifact through the chopper circuit. The chopper is characterized by swift switching behavior, continually alternating direction when receiving input signals from both ends. It results in converting low-frequency signals into high-frequency signals. Assuming the signal of interest to be a differential LFP signal, it undergoes rapid switching, alternating between the P and N terminals. As a result, this signal is modulated into a high-frequency chopping frequency signal, often at frequencies such as 6 kHz or

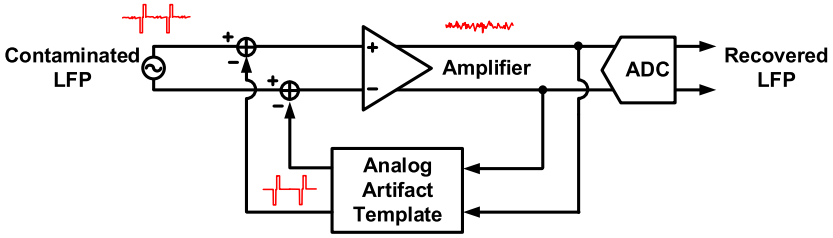

FIGURE 7. Block diagram of template removal in analog domain.

32 kHz. Significantly, the switching process does not alter the frequency of the artifact itself, for example, a stimulation frequency of 130 Hz. Under the circumstances, this technique shifts the frequency of the signal of interest to a range significantly distant from the artifacts. Following the input chopper, in collaboration with clamping diodes, voltage release is limited, effectively clamping high-voltage CMAV to prevent amplifier saturation. Subsequently, demodulation is performed to switch the high-frequency signal of interest to its original frequency.

The DMAV removal is accomplished by utilizing the template removal in analog domain technique [33]. A feedback capacitor circuit is employed for each comparison to assess whether the DMAV possesses a positive or negative polarity. After polarity determination, a compensation circuit located at the input end gradually applies for compensation, bit by bit. The result of this compensation process is a predetermined template. For instance, in cases where the stimulation exhibits a biphasic waveform, as shown in Fig. 2, comprising both a negative and a positive square wave, the input circuit is configured to generate a negative and a positive biphasic waveform, followed by a gradual bit-by-bit compensation process at the input end. However, if the actual artifacts significantly deviate from the preset template, the efficacy of DMAV removal may be compromised. The advantage of this circuit lies in its capability to handle both CMAV and DMAV, featuring a generous CMAV allowable range ($\pm$ 1 V) and a moderate DMAV allowable range ($\pm$ 30 mV). As such, it proves well-suited for implantable closed-loop DBS applications.

The advantage of the template removal in analog domain technique lies in its ability to remove both CMAV and DMAV within the AFE stage, ensuring that the AFE amplifier remains unaffected by CMAV-induced saturation [33]. Besides, the process of template training requires minimal computational effort so this technique is suitable in implantable closed-loop DBS systems. Additionally, the chip area required is smaller due to the absence of a need for supplementary digital filters. However, the disadvantage of this technique lies in the demand for a sophisticated circuit design to address asymmetric DMAV [33]. In addition, the precision of the analog template is comparatively lower than that of the digital template. Furthermore, in scenarios where the stimulation waveform is intricate, the artifact shape is unconventional, or the artifact exhibits consistent alterations, the effectiveness of template removal in analog domain may diminish.

C. BLANKING

The third technique for artifact removal is the utilization of the blanking technique [44], [45]. The fundamental concept involves the direct closure of the input pathway during stimulation-induced artifact occurrence. The AFE amplifiers are reset and disengaged from the electrodes throughout the stimulation period [44]. A block diagram depicting the blanking technique is presented in Fig. 8. As illustrated in Fig. 9, presuming the sine wave represents the signal of interest and the stimulation signal comprises a biphasic square wave artifact. Complete blanking entails resetting the input end from the first stimulation pulse to the last. Sensing operations are halted, resulting in the loss of the entire signal. Within the blanking technique, sensing is interrupted, leading to the loss of the signal of interest.

In [44], the amplifier and acquisition circuit are reset during blanking. The sensor is reactivated following stimulation, but the amplifier requires a reset operation to reestablish a steady state. This stabilization process entails a duration exceeding 3 ms. Despite the brief duration of a stimulation pulse at 150 μs, a certain amount of time is required for recovery following complete blanking before the system can resume sensing a signal. Consequently, an extended signal gap occurs, with considerable periods of signal loss.

The advantage of this technique is that the artifact voltage exerts no detrimental influence on the internal circuitry, thereby averting amplifier saturation [40]. The essential circuitry is spared from addressing the detrimental impacts of artifact voltages, so the design and execution of the circuit are comparatively straightforward. The blanking circuit can be accomplished by incorporating a switch, eliminating the necessity for additional high-power consumption or offline operations. The main disadvantage of blanking is the extended recovery period following stimulation [46], [49]. This outcome contributes to discontinuities within the recorded data, potentially compromising signal linearity. The realization of implantable closed-loop DBS becomes unattainable during blanking periods.

D. SELECTIVE SAMPLING

The fourth technique involves the utilization of the selective sampling technique [22], [32], [46]. The core concept involves synchronizing the sampling clock of the circuit with the stimulation pulses to ensure that the artifact voltages are never subjected to sampling. Typically, selective sampling is implemented through a system-on-a-chip (SoC)

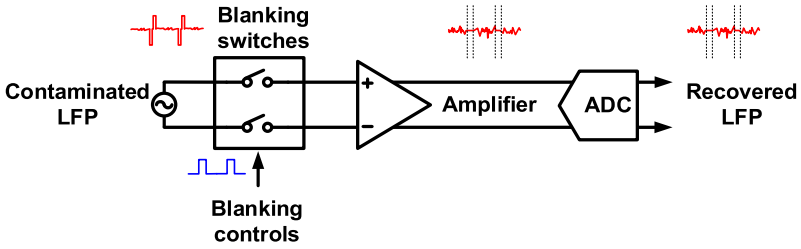

FIGURE 8. Block diagram of blanking.

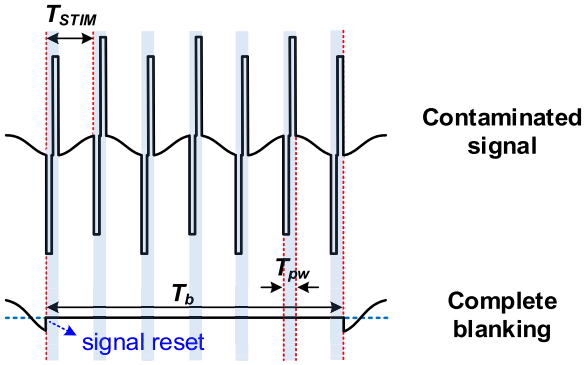

FIGURE 9. Complete blanking.

design, enabling the synchronous control of both the stimulator and ADC sampling processes. This involves calculating the stimulation frequency and sampling frequency and then staggering the number of sampling points and stimulation pulses to ensure that the collected data avoids sampling the stimulation waveform. In this manner, the objective of artifact removal is accomplished. The selective sampling technique can be realized either in digital domain [22], [46] or in analog domain [32].

1) SELECTIVE SAMPLING IN DIGITAL DOMAIN

In the digital domain, selective sampling involves the computation of the relationship between the sampling frequency and stimulation frequency multiples during the system design phase. The ADC can ensure that no artifact voltages are sampled, as depicted in Fig. 10. The technique is also called irregular sampling [22]. This technique facilitates artifact removal within the digital domain without additional operations. The successful implementation of selective sampling relies on accurately determining the common multiple. Nevertheless, this technique is executed after the amplification stage. Given that selective sampling occurs in digital domain, CMAV may lead to output saturation within the AFE amplifier. The primary limitation of this technique pertains to common-mode artifacts [32], [46]. Although selective sampling in digital domain can effectively achieve artifact voltage removal, it proves unsuitable for implantable closed-loop DBS system applications, primarily due to its inability for CMAV removal.

2) SELECTIVE SAMPLING IN ANALOG DOMAIN

An enhanced variation of selective sampling in analog domain within the AFE stage is introduced as the synchronized sample-and-hold artifact blanking (SSAB) technique in [32]. As depicted in Fig. 11, SSAB combines the principles of blanking and selective sampling, primarily leveraging blanking to obstruct the entry of stimulation-induced artifacts into the input end. The timing of blanking aligns with the stimulation control signal. Before the stimulation arrives at the input end and before deactivating the detection circuit, the detected signal is stored on the capacitor within the amplifier input end. Throughout the stimulation phase, the AFE amplifier is held in position without resetting to zero (as shown in Fig. 12). Consequently, it can be conveniently reactivated after the stimulation ends. Furthermore, compared to the alterations in stimulation, changes in the LFP signal occur comparatively slowly. This characteristic ensures that the potential difference remains relatively limited before and after stimulation, facilitating a quicker recovery speed.

The advantage of selective sampling in analog domain lies in its fusion of selective sampling and blanking techniques, preventing the AFE amplifier output from saturation due to substantial CMAV [32]. It enables artifact removal, facilitating the realization of implantable closed-loop DBS systems. However, a disadvantage associated with this technique is that it constrains the stimulation pulse duration [32]. Prolonged stimulation pulses may result in the persistence of output signal discontinuities and a subsequent reduction in linearity.

IV. COMPARISON OF ARTIFACT REMOVAL TECHNIQUES IN IMPLANTABLE CLOSED-LOOP DBS

The feasibility and limitations of implantable closed-loop artifact removal in the DBS are demonstrated in Table 2. The filtering technique requires high-order filters to achieve effective artifact removal, accompanied by considerably high-power consumption, rendering it inappropriate for implementation in implanted systems. Computational demands render template removal in digital domain techniques impractical. On the other hand, the template removal in analog domain technique proves more amenable for implantable artifact removal systems, albeit entailing a relatively intricate system design. The extended recovery time associated with the blanking technique precludes its suitability for closed-loop DBS applications. Selective sampling technique in digital domain fails to remove CMAV, which exhibits a propensity for inducing system saturation.

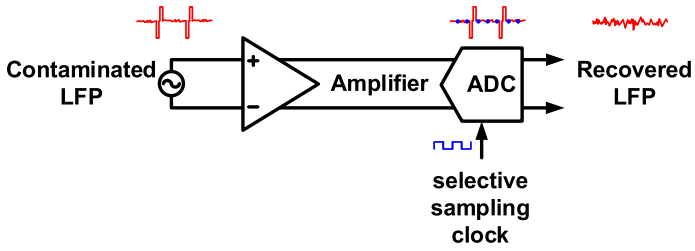

FIGURE 10. Block diagram of selective sampling in digital domain.

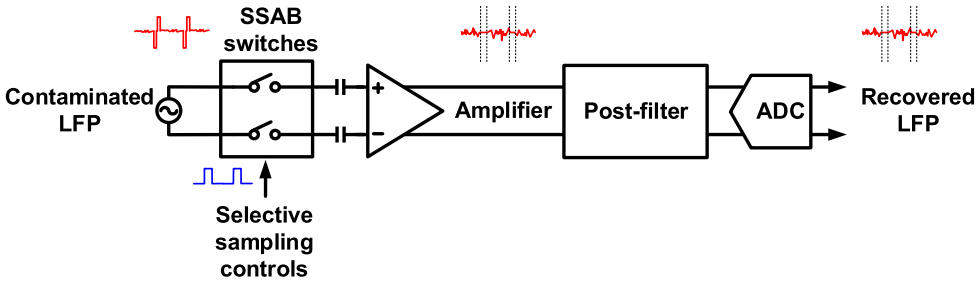

FIGURE 11. Block diagram of selective sampling in analog domain.

TABLE 2. Comparison of artifact removal techniques in the DBS design.

Artifact removal technique		Latency between contaminated LFP and recovered LFP	Extra power consumption of artifact removal design	Implemented in SoC	Suitable for implantable closed-loop DBS system applications
Filtering [31], [34]–[36]		Short/Moderate	Large	No	No
Template Removal	Digital [37]–[42]	Moderate/Long	Large	No	No
	Analog [33], [43]	Moderate	Moderate	Yes	Yes
Blanking [44], [45]		Short	Low	Yes	No
Selective Sampling	Digital [22], [46]	Short	Low	No	No
	Analog [32]	Short	Low	Yes	Yes

In contrast, selective sampling in analog domain emerges as a more fitting option for implantable closed-loop DBS artifact removal.

Although various techniques for artifact voltage removal have been proposed, only template removal in analog domain and selective sampling in analog domain techniques are presently considered suitable for implantable closed-loop DBS system applications, and they have been integrated on-chip within the AFE amplifier. The advantage of SSAB in selective sampling in analog domain is that there is no need to distinguish between CMAV and DMAV, as they can be entirely suppressed. Tolerable levels of DMAV can reach volts. Even when a substantial differential signal mismatch is present, smooth removal remains achievable. Furthermore, SSAB obviates the necessity for additional compensation and comparator circuits, resulting in significantly lower additional power consumption and almost negligible.

Accordingly, both template removal in analog domain and selective sampling in analog domain can be implemented in the SoC for implantable closed-loop DBS applications. Additionally, they have low requirements for additional power consumption. Both template removal in analog domain and selective sampling in analog domain design are notably more appropriate for implantable systems, providing a route to optimal power utilization.

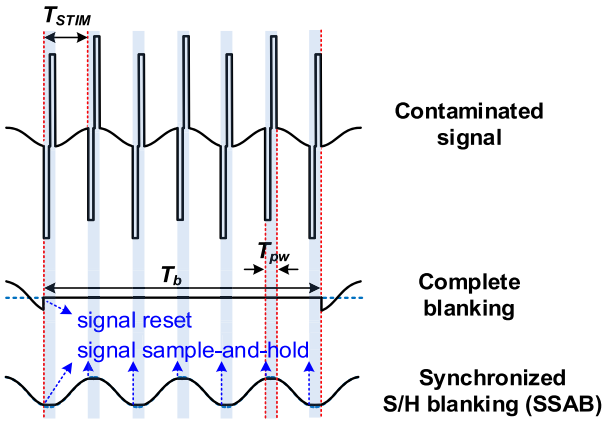

FIGURE 12. Synchronized sample-and-hold artifact blanking (SSAB).

V. CONCLUSION

This article comprehensively reviews the stimulation-induced artifact removal techniques, including filtering, template removal, blanking, and selective sampling. The filtering technique can effectively remove artifacts, but it was accompanied by the limitation where the filter bandwidth constrained the stimulation frequency and the unaffected bio-signal frequency.

The template removal technique can be further divided into digital and analog domains. Template removal in digital domain yields good output results when the artifact waveform template has undergone precise training. However, it can only be utilized when the artifact voltage is not too large or over-saturated. Besides, it requires a lot of computing power consumption, making it challenging to process artifacts in implantable systems. Template removal in analog domain can remove both CMAV and DMAV within the AFE stage, but a sophisticated circuit design is needed to address asymmetric DMAV.

The blanking technique is utilized to deactivate signal detection during stimulation. However, its disadvantages include extended recovery times and discontinuities in the bio-signal, subsequently impacting spectral analysis.

The selective sampling technique can selectively sample the detection signal and avoid the occurrence time of artifacts. It is divided into selective sampling in digital domain and analog domain. Selective sampling in digital domain imposes constraints on the input dynamic range of the amplifier and the resolution of the ADC. Selective sampling in analog domain, implemented as SSAB, combines the blanking and selective sampling techniques to block CMAV and DMAV with a low distortion rate. However, the stimulation pulse width cannot be too long; otherwise, the signal distortion rate will increase.

With an artifact-removal system, researchers can focus on improving detection algorithms and stimulation functions based on movement disorders. Finally, an implantable closed-loop DBS system can be achieved.

ACKNOWLEDGMENT

(Yi-Hui Wu and Hsiao-Chun Lin contributed equally to this work.)

REFERENCES

[1] B. R. Bloem, M. S. Okun, and C. Klein, "Parkinson's disease," *Lancet*, vol. 397, no. 10291, pp. 2284–2303, 2021.
[2] B. S. Connolly and A. E. Lang, "Pharmacological treatment of Parkinson disease: A review," *JAMA*, vol. 311, no. 16, pp. 1670–1683, Apr. 2014.
[3] A. M. Lozano, N. Lipsman, H. Bergman, P. Brown, S. Chabardes, J. W. Chang, K. Matthews, C. C. McIntyre, T. E. Schlaepfer, M. Schulder, Y. Temel, J. Volkmann, and J. K. Krauss, "Deep brain stimulation: Current challenges and future directions," *Nat. Rev. Neurol.*, vol. 15, no. 3, pp. 148–160, Mar. 2019.
[4] W.-J. Neumann, H. Schroll, A. L. de Almeida Marcelino, A. Horn, S. Ewert, F. Irmen, P. Krause, G.-H. Schneider, F. Hamker, and A. A. Kuhn "Functional segregation of basal ganglia pathways in Parkinson's disease," *Brain*, vol. 141, no. 9, pp. 2655–2669, Sep. 2018.
[5] Z. Yin, G. Zhu, B. Zhao, Y. Bai, Y. Jiang, W.-J. Neumann, A. A. Kuhn, and J. Zhang, "Local field potentials in Parkinson's disease: A frequency-based review," *Neurobiol. Disease*, vol. 155, Jul. 2021, Art. no. 105372.
[6] S. Marceglia, M. Guidetti, I. E. Harmsen, A. Loh, S. Meoni, G. Foffani, A. M. Lozano, J. Volkmann, E. Moro, and A. Priori, "Deep brain stimulation: Is it time to change gears by closing the loop?" *J. Neural Eng.*, vol. 18, no. 6, Nov. 2021, Art. no. 061001.
[7] W.-J. Neumann, R. Gilron, S. Little, and G. Tinkhauser, "Adaptive deep brain stimulation: From experimental evidence toward practical implementation," *Movement Disorders*, vol. 38, no. 6, pp. 937–948, Jun. 2023.
[8] W.-J. Neumann, A. Horn, and A. A. Kuhn, "Insights and opportunities for deep brain stimulation as a brain circuit intervention," *Trends Neurosciences*, vol. 46, no. 6, pp. 472–487, Jun. 2023.
[9] S. Little, A. Pogosyan, S. Neal, B. Zavala, L. Zrinzo, M. Hariz, T. Foltynie, P. Limousin, K. Ashkan, J. FitzGerald, A. L. Green, T. Z. Aziz, and P. Brown, "Adaptive deep brain stimulation in advanced Parkinson disease," *Ann. Neurol.*, vol. 74, no. 3, pp. 449–457, Sep. 2013.
[10] S. Little, M. Beudel, L. Zrinzo, T. Foltynie, P. Limousin, M. Hariz, S. Neal, B. Cheeran, H. Cagnan, J. Gratwicke, T. Z. Aziz, A. Pogosyan, and P. Brown, "Bilateral adaptive deep brain stimulation is effective in Parkinson's disease," *J. Neurol. Neurosurg. Psychiat.*, vol. 87, no. 7, pp. 717–721, 2016.
[11] M. Arlotti, L. Rossi, M. Rosa, S. Marceglia, and A. Priori, "An external portable device for adaptive deep brain stimulation (aDBS) clinical research in advanced Parkinson's disease," *Med. Eng. Phys.*, vol. 38, no. 5, pp. 498–505, May 2016.
[12] T. Bocci, M. Prenassi, M. Arlotti, F. M. Cogiamanian, L. Borellini, E. Moro, A. M. Lozano, J. Volkmann, S. Barbieri, A. Priori, and S. Marceglia, "TU-197. eight-hours conventional versus adaptive deep brain stimulation of the subthalamic nucleus (STN) in Parkinson's disease," *NPJ Parkinsons Dis.*, vol. 7, no. 1, Sep. 2021, Art. no. 88.
[13] A. Velisar, J. Syrkin-Nikolau, Z. Blumenfeld, M. H. Trager, M. F. Afzal, V. Prabhakar, and H. Bronte-Stewart, "Dual threshold neural closed loop deep brain stimulation in Parkinson disease patients," *Brain Stimulation*, vol. 12, no. 4, pp. 868–876, Jul. 2019.
[14] M. N. Petrucci, R. S. Neuville, M. F. Afzal, A. Velisar, C. M. Anidi, R. W. Anderson, J. E. Parker, J. J. O'Day, K. B. Wilkins, and H. M. Bronte-Stewart, "Neural closed-loop deep brain stimulation for freezing of gait," *Brain Stimulation*, vol. 13, no. 5, pp. 1320–1322, Sep. 2020.
[15] W. Bouthour, P. Mégevand, J. Donoghue, C. Luscher, N. Birbaumer, and P. Krack, "Biomarkers for closed-loop deep brain stimulation in Parkinson disease and beyond," *Nature Rev. Neurol.*, vol. 15, no. 6, pp. 343–352, Jun. 2019.
[16] S. Little and P. Brown, "The functional role of beta oscillations in Parkinson's disease," *Parkinsonism Rel. Disorders*, vol. 20, pp. S44–S48, Jan. 2014.
[17] G. Giannicola, S. Marceglia, L. Rossi, S. Mrakic-Sposta, P. Rampini, F. Tamma, F. Cogiamanian, S. Barbieri, and A. Priori, "The effects of levodopa and ongoing deep brain stimulation on subthalamic beta oscillations in Parkinson's disease," *Experim. Neurol.*, vol. 226, no. 1, pp. 120–127, Nov. 2010.
[18] A. A. Kuhn, F. Kempf, C. Brucke, L. Gaynor Doyle, I. Martinez-Torres, A. Pogosyan, T. Trottenberg, A. Kupsch, G.-H. Schneider, M. I. Hariz, W. Vandenberghe, B. Nuttin, and P. Brown, "High-frequency stimulation of the subthalamic nucleus suppresses oscillatory beta activity in patients with Parkinson's disease in parallel with improvement in motor performance," *J. Neurosci.*, vol. 28, no. 24, pp. 6165–6173, Jun. 2008.
[19] S. Wang, G. Zhu, L. Shi, C. Zhang, B. Wu, A. Yang, F. Meng, Y. Jiang, and J. Zhang, "Closed-loop adaptive deep brain stimulation in Parkinson's disease: Procedures to achieve it and future perspectives," *J. Parkinson's Disease*, vol. 13, no. 4, pp. 453–471, Jun. 2023.

[20] N. C. Swann, C. de Hemptinne, M. C. Thompson, S. Miocinovic, A. M. Miller, R. Gilron, J. L. Ostrem, H. J. Chizeck, and P. A. Starr, "Adaptive deep brain stimulation for Parkinson's disease using motor cortex sensing," *J. Neural Eng.*, vol. 15, no. 4, Aug. 2018, Art. no. 046006.

[21] J. K. Krauss, N. Lipsman, T. Aziz, A. Boutet, P. Brown, J. W. Chang, B. Davidson, W. M. Grill, M. I. Hariz, A. Horn, M. Schulder, A. Mammis, P. A. Tass, J. Volkmann, and A. M. Lozano, "Technology of deep brain stimulation: Current status and future directions," *Nature Rev. Neurol.*, vol. 17, no. 2, pp. 75–87, Feb. 2021.

[22] Y. Nie, X. Guo, X. Li, X. Geng, Y. Li, Z. Quan, G. Zhu, Z. Yin, J. Zhang, and S. Wang, "Real-time removal of stimulation artifacts in closed-loop deep brain stimulation," *J. Neural Eng.*, vol. 18, no. 6, Dec. 2021, Art. no. 066031.

[23] G. Tinkhauser, A. Pogosyan, S. Little, M. Beudel, D. M. Herz, H. Tan, and P. Brown, "The modulatory effect of adaptive deep brain stimulation on beta bursts in Parkinson's disease," *Brain*, vol. 140, no. 4, pp. 1053–1067, Apr. 2017.

[24] T. M. Frasczek, B. I. Ferleger, T. E. Brown, M. C. Thompson, A. J. Haddock, B. C. Houston, J. G. Ojemann, A. L. Ko, J. A. Herron, and H. J. Chizeck, "Closing the loop with cortical sensing: The development of adaptive deep brain stimulation for essential tremor using the activa PC+S," *Frontiers Neurosci.*, vol. 15, Dec. 2021, Art. no. 749705.

[25] D. R. Merrill, M. Bikson, and J. G. R. Jefferys, "Electrical stimulation of excitable tissue: Design of efficacious and safe protocols," *J. Neurosci. Methods*, vol. 141, no. 2, pp. 171–198, Feb. 2005.

[26] S. F. Cogan, "Neural stimulation and recording electrodes," *Annu. Rev. Biomed. Eng.*, vol. 10, pp. 275–309, Aug. 2008.

[27] S. F. Cogan, K. A. Ludwig, C. G. Welle, and P. Takmakov, "Tissue damage thresholds during therapeutic electrical stimulation," *J. Neural Eng.*, vol. 13, no. 2, Apr. 2016, Art. no. 021001.

[28] M. Katebi, A. Erfanian, M. Azim Karami, and M. Sawan, "Challenges and trends of implantable functional electrical neural stimulators: System architecture and parameters," *IEEE Access*, vol. 12, pp. 103203–103236, 2024.

[29] S. Abdollahifard, A. Farrokhi, S. Mosalamiaghili, K. Assadian, O. Yousefi, and A. Razmkon, "Constant current or constant voltage deep brain stimulation: Short answers to a long story," *Acta Neurologica Belgica*, vol. 123, no. 1, pp. 1–8, Feb. 2023.

[30] C.-C. Hsieh, Y.-H. Wu, and M.-D. Ker, "Design of dual-configuration dual-mode stimulator in low-voltage CMOS process for neuromodulation," *IEEE Trans. Biomed. Circuits Syst.*, vol. 17, no. 2, pp. 273–285, Apr. 2023.

[31] L. Rossi, G. Foffani, S. Marceglia, F. Bracchi, S. Barbieri, and A. Priori, "An electronic device for artefact suppression in human local field potential recordings during deep brain stimulation," *J. Neural Eng.*, vol. 4, no. 2, pp. 96–106, Jun. 2007.

[32] C.-W. Huang, C.-K. Lai, C.-C. Hung, C.-Y. Wu, and M.-D. Ker, "A CMOS synchronized sample-and-hold artifact blanking analog front-end local field potential acquisition unit with ±3.6-V stimulation artifact tolerance and monopolar electrode-tissue impedance measurement circuit for closed-loop deep brain stimulation SoCs," *IEEE Trans. Circuits Syst. I, Reg. Papers*, vol. 70, no. 6, pp. 2257–2270, Jun. 2023.

[33] C.-Y. Wu, C.-W. Huang, Y.-W. Chen, C.-K. Lai, C.-C. Hung, and M.-D. Ker, "Design of CMOS analog front-end local-field potential chopper amplifier with stimulation artifact tolerance for real-time closed-loop deep brain stimulation SoC applications," *IEEE Trans. Biomed. Circuits Syst.*, vol. 18, no. 3, pp. 539–551, Jun. 2024.

[34] H. Chandrakumar and D. Markovic, "An 80-mVpp linear-input range, 1.6-GΩ input impedance, low-power chopper amplifier for closed-loop neural recording that is tolerant to 650-mVpp common-mode interference," *IEEE J. Solid-State Circuits*, vol. 52, no. 11, pp. 2811–2828, Nov. 2017.

[35] K. Petkos, T. Guiho, P. Degenaar, A. Jackson, P. Brown, T. Denison, and E. M. Drakakis, "A high-performance 4 nV $(\sqrt{\text{Hz}})^{-1}$ analog front-end architecture for artefact suppression in local field potential recordings during deep brain stimulation," *J. Neural Eng.*, vol. 16, no. 6, Oct. 2019, Art. no. 066003.

[36] S. Stanslaski, P. Afshar, P. Cong, J. Giftakis, P. Stypulkowski, D. Carlson, D. Linde, D. Ullestad, A.-T. Avestruz, and T. Denison, "Design and validation of a fully implantable, chronic, closed-loop neuromodulation device with concurrent sensing and stimulation," *IEEE Trans. Neural Syst. Rehabil. Eng.*, vol. 20, no. 4, pp. 410–421, Jul. 2012.

[37] Y. Wang, H. Luo, Y. Chen, Z. Jiao, Q. Sun, L. Dong, X. Chen, X. Wang, and H. Zhang, "A closed-loop neuromodulation chipset with 2-level classification achieving 1.5-vpp CM interference tolerance, 35-dB stimulation artifact rejection in 0.5ms and 97.8%-sensitivity seizure detection," *IEEE Trans. Biomed. Circuits Syst.*, vol. 15, no. 4, pp. 802–819, Aug. 2021.

[38] D. Rozgic, V. Hokhikyan, W. Jiang, I. Akita, S. Basir-Kazeruni, H. Chandrakumar, and D. Markovic, "A 0.338 cm^3, artifact-free, 64-contact neuromodulation platform for simultaneous stimulation and sensing," *IEEE Trans. Biomed. Circuits Syst.*, vol. 13, no. 1, pp. 38–55, Feb. 2019.

[39] X. Qian, Y. Chen, Y. Feng, B. Ma, H. Hao, and L. Li, "A method for removal of deep brain stimulation artifact from local field potentials," *IEEE Trans. Neural Syst. Rehabil. Eng.*, vol. 25, no. 12, pp. 2217–2226, Dec. 2017.

[40] A. Zhou, S. R. Santacruz, B. C. Johnson, G. Alexandrov, A. Moin, F. L. Burghardt, J. M. Rabaey, J. M. Carmena, and R. Müller, "A wireless and artefact-free 128-channel neuromodulation device for closed-loop stimulation and recording in non-human primates," *Nature Biomed. Eng.*, vol. 3, no. 1, pp. 15–26, Dec. 2018.

[41] J. P. Uehlin, W. A. Smith, V. R. Pamula, S. I. Perlmutter, J. C. Rudell, and V. S. Sathe, "A 0.0023 mm^2/ch. delta-encoded, time-division multiplexed mixed-signal ECoG recording architecture with stimulus artifact suppression," *IEEE Trans. Biomed. Circuits Syst.*, vol. 14, no. 2, pp. 319–331, Apr. 2020.

[42] A. Samiei and H. Hashemi, "A bidirectional neural interface SoC with adaptive IIR stimulation artifact cancelers," *IEEE J. Solid-State Circuits*, vol. 56, no. 7, pp. 2142–2157, Jul. 2021.

[43] P.-W. Chen, F.-Y. Tu, and C.-Y. Wu, "A chopper-stabilized 65nm CMOS analog front-end acquisition circuit with high-linearity low-power switched-capacitor filter/amplifier for EEG recording," in *Proc. Int. Conf. Analog VLSI Circuits*, 2019, pp. 1–20.

[44] R. A. Blum, J. D. Ross, E. A. Brown, and S. P. DeWeerth, "An integrated system for simultaneous, multichannel neuronal stimulation and recording," *IEEE Trans. Circuits Syst. I, Reg. Papers*, vol. 54, no. 12, pp. 2608–2618, Dec. 2007.

[45] C.-Y. Wu, C.-H. Cheng, and Z.-X. Chen, "A 16-channel CMOS chopper-stabilized analog front-end ECoG acquisition circuit for a closed-loop epileptic seizure control system," *IEEE Trans. Biomed. Circuits Syst.*, vol. 12, no. 3, pp. 543–553, Jun. 2018.

[46] J. Debarros, L. Gaignon, S. He, A. Pogosyan, M. Benjaber, T. Denison, P. Brown, and H. Tan, "Artefact-free recording of local field potentials with simultaneous stimulation for closed-loop deep-brain stimulation," in *Proc. 42nd Annu. Int. Conf. IEEE Eng. Med. Biol. Soc. (EMBC)*, Jul. 2020, pp. 3367–3370.

[47] A. Zhou, B. C. Johnson, and R. Müller, "Toward true closed-loop neuromodulation: Artifact-free recording during stimulation," *Current Opinion Neurobiol.*, vol. 50, pp. 119–127, Jun. 2018.

[48] T. Hashimoto, C. M. Elder, and J. L. Vitek, "A template subtraction method for stimulus artifact removal in high-frequency deep brain stimulation," *J. Neurosci. Methods*, vol. 113, no. 2, pp. 181–186, Jan. 2002.

[49] S. F. Lempka, B. Howell, K. Gunalan, A. G. Machado, and C. C. McIntyre, "Characterization of the stimulus waveforms generated by implantable pulse generators for deep brain stimulation," *Clin. Neurophysiol.*, vol. 129, no. 4, pp. 731–742, Apr. 2018.

YI-HUI WU received the B.S. degree from the Department of Physical Therapy, Kaohsiung Medical University, Kaohsiung, Taiwan, in 2002, and the Ph.D. degree from the Graduate Institute of Electrical Engineering, National Taiwan University, Taipei, Taiwan, in 2008. She was with the Office of Medical Device Evaluation, Center for Measurement Standards, Industrial Technology Research Institute, Hsinchu, Taiwan, from 2008 to 2016. She is currently a Postdoctoral Researcher with the Biomedical Electronics Translational Research Center, National Yang Ming Chiao Tung University, Hsinchu. Her current research interests include signal processing of closed-loop DBS systems, biomedical signal analysis, neuromodulation system implementation, and medical device regulations.

HSIAO-CHUN LIN received the Ph.D. degree from the Department of Life Science, National Taiwan University, in 2014. His expertise is in electrophysiology, neuroanatomy, and animal models of brain disease. He is currently an Assistant Research Fellow with the Biomedical Electronics Translational Research Center, National Yang Ming Chiao Tung University, Hsinchu. His research interests include the treatment of neurodegenerative diseases through invasive or non-invasive electrical brain stimulation, such as deep brain stimulation to treat Parkinson's disease or transcranial electrical stimulation to treat Alzheimer's disease.

CHI-WEI HUANG received the B.S. degree from the Department of Electrical Engineering and Computer Science Honors Program, National Chiao Tung University, Hsinchu, Taiwan, in 2016, and the Ph.D. degree from the Institute of Electronics, National Yang Ming Chiao Tung University, Hsinchu, in 2024. He is currently a Researcher with the Biomedical Electronics Translational Research Center, National Yang Ming Chiao Tung University, and an Engineer in A-Neuron Electronic Corporation, Hsinchu. His research interests include CMOS low noise amplifier design, stimulation artifact removal techniques, mixed-signal system integration, closed-loop DBS systems, and biomedical electronics.

CHUNG-YU WU (Life Fellow, IEEE) was born in 1950. He received the M.S. and Ph.D. degrees from the Department of Electronics Engineering, National Chiao Tung University, Hsinchu, Taiwan, in 1976 and 1980, respectively. Since 1980, he has been a consultant to high-tech industry and research organizations and has built up strong research collaborations with high-tech industries. From 1980 to 1983, he was an Associate Professor with National Chiao Tung University. From 1984 to 1986, he was a Visiting Associate Professor with the Department of Electrical Engineering, Portland State University, Portland, OR, USA. Since 1987, he has been a Professor with National Chiao Tung University. From 1991 to 1995, he was rotated to serve as the Director of the Division of Engineering and Applied Science, National Science Council, Taipei, Taiwan. From 1996 to 1998, he was honored as the Centennial Honorary Chair Professor of National Chiao Tung University. He received the National Chair Professorship (2015–2017) from the Ministry of Education. He is currently an Emeritus Chair Professor with National Yang Ming Chiao Tung University, Hsinchu, and the Chairperson/CTO of A-Neuron Electronic Corporation, Hsinchu. He has published more than 300 technical papers in international transactions/journals and conferences. He holds 56 patents, including 23 U.S. patents. His research interests include implantable biomedical integrated circuits and systems, intelligent bioinspired sensor systems, RF/microwave communication integrated circuits, neural networks, analog/mixed-signal integrated circuits, and nanoelectronics. He is also a member of the Eta Kappa Nu and Phi Tau Phi Honorary Scholastic societies. He was a recipient of the IEEE Fellow Award in 1998, the Third Millennium Medal in 2000, and the IEEE Life Fellow Award in 2020. In Taiwan, he received numerous research awards from the Ministry of Education, National Science Council, and professional foundations.

MING-DOU KER (Fellow, IEEE) received the Ph.D. degree from the Institute of Electronics, National Chiao Tung University (NCTU), Hsinchu, Taiwan, in 1993.

In 2015, he was the Dean of the College of Photonics, NCTU. He was the Department Manager of the VLSI Design Division, Industrial Technology Research Institute, Hsinchu. He was the Director of the Institute of Pioneer Semiconductor Innovation, National Yang Ming Chiao Tung University, Hsinchu, from 2022 to 2023, where he is currently a Chair Professor with the Institute of Electronics, the Director of the Biomedical Electronics Translational Research Center, the Associate Dean of the College of Electrical and Computer Engineering, and the Chairperson of the Department of Microelectronics. In the technical field of reliability and quality design for microelectronic circuits and systems, he has authored/co-authored over 640 technical papers in international journals and conferences. He has proposed many solutions to improve the reliability and quality of integrated circuits, which have been granted with hundreds of U.S. patents. He had been invited to teach and/or to consult the reliability and quality design by hundreds of design houses and semiconductor companies in the worldwide IC industry. Some of his inventions or designs had been widely used in the modern IC products and the microelectronic systems. His current research interests include the circuits and systems for biomedical applications and the reliability design for nanoelectronics and gigascale systems.

Prof. Ker served as a member for the Technical Program Committee and the Session Chair for numerous international conferences for many years, including the IEEE International Symposium on VLSI Technology and Circuits, the IEEE International Solid-State Circuits Conference, the IEEE International Symposium on Circuits and Systems, and the IEEE International Reliability Physic Symposium. He has been a fellow of Chinese Institute of Electrical Engineering. He served as the Distinguished Lecturer for the IEEE Circuits and Systems Society from 2006 to 2007 and the IEEE Electron Devices Society from 2008 to 2020. He was an Associate Editor of IEEE TRANSACTIONS ON VERY LARGE SCALE INTEGRATION SYSTEMS and IEEE TRANSACTIONS ON BIOMEDICAL CIRCUITS AND SYSTEMS and the Guest Editor of *Frontiers in Neuroscience* on the research topic of microelectronic implants for central and peripheral nervous systems, and IEEE TRANSACTIONS ON ELECTROMAGNETIC COMPATIBILITY of the Special Issue on "Electrostatic Discharge and Immunity–from IC to System." He was the Founding President of Taiwan ESD Association, the 3rd President of Taiwan Engineering Medicine Biology Association, and the 21th Vice-President of IEEE Taipei Section. He is currently serving as an Editor for IEEE TRANSACTIONS ON DEVICE AND MATERIALS RELIABILITY and IEEE JOURNAL OF THE ELECTRON DEVICES SOCIETY.